





Cite this: *RSC Adv.*, 2025, 15, 17379

# Structural and FTIR spectroscopic studies of matrix-isolated 3-thio-1,2,4-triazole complexes with carbon dioxide. The UV-induced formation of thiol...CO<sub>2</sub> complexes†

Karolina Mucha, \* Magdalena Pagacz-Kostrzewa  and Maria Wierzejewska 

Matrix isolation FTIR spectroscopy was combined with quantum chemical calculations to characterize complexes of 3-thio-1,2,4-triazole (ST) with carbon dioxide. Geometries of the possible 1:1 and 1:2 complexes were optimized at the DFT (B3LYPD3) level of theory with the 6-311++G(3df,3pd) basis set. The computational results show that ST interacts specifically with carbon dioxide through different hydrogen bond and van der Waals interactions. For the 1:1 complexes of the most abundant ST thione tautomer, four stable minima, ST $n$ ...CO<sub>2</sub>, have been located on the potential energy surface. In contrast, for the ST thiol tautomer, three STl...CO<sub>2</sub> structures were optimized. Experimentally, the two most stable 1:1 complexes of ST $n$  with CO<sub>2</sub>, characterized by the presence of the N-H...O hydrogen bridge and an additional S6...C10 interaction, were identified in solid argon upon deposition. Annealing of the matrix at 32 K proved that one 1:2 structure is also present, resulting from the addition of a second CO<sub>2</sub> molecule to the 1:1 complexes. The laser irradiation at  $\lambda = 270$  nm, apart from generating the thiol tautomer of ST, also leads to the formation of three thiol...CO<sub>2</sub> complexes. Furthermore, the presence of CO<sub>2</sub> in the argon matrix was found to influence the efficiency of the UV-induced thione–thiol tautomerization, though to a lesser extent than nitrogen. This suggests that while CO<sub>2</sub> forms stronger intermolecular interactions with ST, its impact on tautomerization kinetics is less pronounced, highlighting the nuanced role of specific gas-phase interactions in modulating photochemical transformations in low-temperature matrices. The findings presented in this work not only enhance the fundamental understanding of weak intermolecular interactions but also provide new insights into the role of CO<sub>2</sub>-specific effects in photochemical and structural transformations of heterocycles.

Received 31st March 2025

Accepted 23rd April 2025

DOI: 10.1039/d5ra02230d

rsc.li/rsc-advances

## 1. Introduction

Intermolecular interactions have been the subject of study for many years and have been examined by a wide variety of techniques. The interest in this area is related to the prevalence of this behavior in nature (*e.g.* biochemical processes,<sup>1,2</sup> the atmosphere,<sup>3,4</sup> surface science,<sup>5</sup> *etc.*). Moreover, in recent years, there has been a great deal of interest in the interactions of various heterocyclic molecules with carbon dioxide. This is related to the role that CO<sub>2</sub> plays in the greenhouse effect and the efforts to establish efficient methods for capturing various atmospheric pollutants. Heterocycles, with their diverse electronic and structural properties, offer a promising foundation for developing functional frameworks that selectively bind and

sequester CO<sub>2</sub>. A group of compounds that are particularly suited for this purpose are azoles, whose applications have been proven by numerous scientific articles regarding the use of those molecules as MOF, MOP, ZIF, or other frameworks' components.<sup>6–10</sup> The subject of this work, 3-thio-1,2,4-triazole (ST), makes a relevant candidate for capturing CO<sub>2</sub> and other pollutants due to the presence of electronegative nitrogen atoms in the ring as well as a thiol group, which creates several possibilities for the acceptor molecule to attach. Another interesting feature of this molecule is its ability to undergo thione–thiol tautomerization, which has been the subject of research due to the importance of heterocyclic tautomerism in various processes related to bioactivity.<sup>11–14</sup> Recent studies have demonstrated that photo-induced tautomerization, such as keto–enol transitions, can alter the electron density distribution of a molecule and subsequently modify the binding affinity and geometry of CO<sub>2</sub> complexes, as shown for carbonyl systems under UV exposure.<sup>15</sup>

Based on our previous work on 3-thio-1,2,4-triazole (ST) complexes with dinitrogen,<sup>16</sup> where we demonstrated different

Faculty of Chemistry, University of Wrocław, F. Joliot-Curie 14, 50-383 Wrocław, Poland. E-mail: karolina.mucha@uw.edu.pl

† Electronic supplementary information (ESI) available: Selected AIM parameters, selected wavenumber shifts, and band intensities of ST...CO<sub>2</sub> complexes calculated at B3LYP-D3/6-311++G(3df,3pd) level. See DOI: <https://doi.org/10.1039/d5ra02230d>



ways of binding  $N_2$  molecules by the azole and identified particular geometries spectroscopically, we decided to study ST- $CO_2$  complexes in a similar way and compare their interaction energies, geometries, and vibrational spectra. Unlike  $N_2$ , which is chemically inert and interacts primarily through dispersion forces and weak hydrogen bonding,  $CO_2$  exhibits a higher degree of electronic polarizability, leading to stronger and more directional interactions with ST. Therefore,  $CO_2$  may serve as a modulator of reaction pathways by stabilizing particular conformations or influencing the energy barriers for tautomerization and photolysis. Changes in the matrix environment may influence the tautomeric equilibrium of heterocyclic compounds as well as the efficiency of UV-induced transformations, which has been documented in the literature in previous years.<sup>17–19</sup> The investigation of ST- $CO_2$  complexes introduces new aspects that significantly extend our understanding of intermolecular interactions in matrix isolation.

## 2. Experimental

### 2.1. Theoretical studies

All computations in this work were performed using the Gaussian 16 suite of quantum chemical programs.<sup>20</sup> The structures of the monomers and the 3-thio-1,2,4-triazole complexes with  $CO_2$  were created in the GaussView 6.0 program<sup>21</sup> and then optimized at the B3LYP-D3/6-311++G(3df,3pd) level of theory<sup>22–26</sup> with the Boys–Bernardi full counterpoise method by Dannenberg *et al.*<sup>27,28</sup> Interaction energies ( $E_{int}$ ) were calculated by subtracting the total electronic energies of the monomers from the energy of the complex while preserving the geometry of the complex. Vibrational wavenumbers were determined using the harmonic approximation to verify that the identified structures correspond to minima on the potential energy surfaces and to monitor spectral changes resulting from the complex formation. To account for anharmonicity, the calculated wavenumbers were scaled by factors of 0.951 for the 4000–2800  $cm^{-1}$  range and 0.982 for the 2800–400  $cm^{-1}$  range. Interactions between ST and  $CO_2$  in complexes were characterized using topological analysis of electron density (AIM),<sup>29,30</sup> which was conducted at the B3LYP-D3/6-311++G(3df,3pd) level with the AIM Studio program (Version 19.10.12, Professional).<sup>31</sup>

### 2.2. Matrix isolation experiments

The preparation of cryogenic matrices was carried out using methods and equipment as described in our previous paper on ST complexes.<sup>16</sup> Carbon dioxide used to prepare  $CO_2$ /Ar matrix gas mixtures was synthesized in the laboratory, and the procedure was described in ref. 32 in section 2.2. The  $CO_2$ /Ar concentrations obtained in the matrix were 1/500 and 1/1000. Photochemical processes were induced in ST/ $CO_2$ /Ar matrices by UV radiation ( $\lambda = 270$  nm) of a pulsed optical parametric oscillator Vibrant (Opotek, Inc.) pumped with a pulsed Nd:YAG laser (Quantel). The progress of the deposition and UV-induced reactions were monitored by recording successive IR spectra.

## 3. Results and discussion

The monomer of 3-thio-1,2,4-triazole (ST) in the matrix isolation conditions appears in the form of thione tautomer (STn) with trace amounts of the thiol tautomer (STl), as described by Rostkowska *et al.*<sup>33</sup> Therefore, considering the complexation of ST with carbon dioxide, only those two structures were taken into account. They are presented in Fig. 1 below, together with the adopted numbering of atoms.

### 3.1. Quantum chemical calculations

**3.1.1. Complexes of the 1:1 stoichiometry.** Using the B3LYP-D3/6-311++G(3df,3pd) method, four STn $\cdots CO_2$  structures and three STl $\cdots CO_2$  structures were optimized. They are presented in Fig. 2 together with the atom numbering as well as calculated values of the interaction energy  $E_{int}$  and relative electronic energy  $\Delta E$ . Selected geometric parameters: bond lengths and angle values and key topological data generated by AIM calculations are given in Tables S1 and S2 in the ESI.<sup>†</sup> Since the thione and thiol forms differ only in the position of one of the hydrogen atoms, the optimized geometries of the complexes of both tautomers are similar. Therefore, it is possible to distinguish analogous structures in both groups. They are marked with the same number (STn-C1 and STl-C1, STn-C2 and STl-C2, STn-C4 and STl-C4). The thiol equivalent of the STn-C3 complex could not be optimized, as it appeared as a very shallow minimum that undergoes a barrierless transformation into the more stable STl-C4 structure. In the first pair of complexes, STn-C1 and STl-C1, the subunits are connected by a hydrogen bond bridge N1-H9 $\cdots$ O11, the angle of which equals 148.6 and 139.0°, respectively. The difference in the values of this angle results from the different position of the  $CO_2$  molecule relative to the triazole ring. In the structure of STn-C1, it lies in the plane, while in the case of STl-C1 it is tilted out of the plane.

In both complexes, there are also additional van der Waals interactions formed between the sulfur atom of the substituent and one of the atoms of the  $CO_2$  molecule. In the case of STn-C1, it is a carbon atom, and in STl-C1, it is an oxygen atom. Interestingly, the interaction energy value calculated for the thione form complex is significantly higher than for the second complex (−22.1  $kJ\ mol^{-1}$  compared to −14.8  $kJ\ mol^{-1}$ ). This is most likely because in STn-C1, the geometry is stabilized by

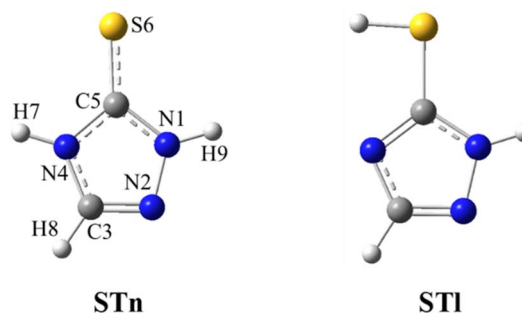


Fig. 1 Structures of thione and thiol tautomers of ST.



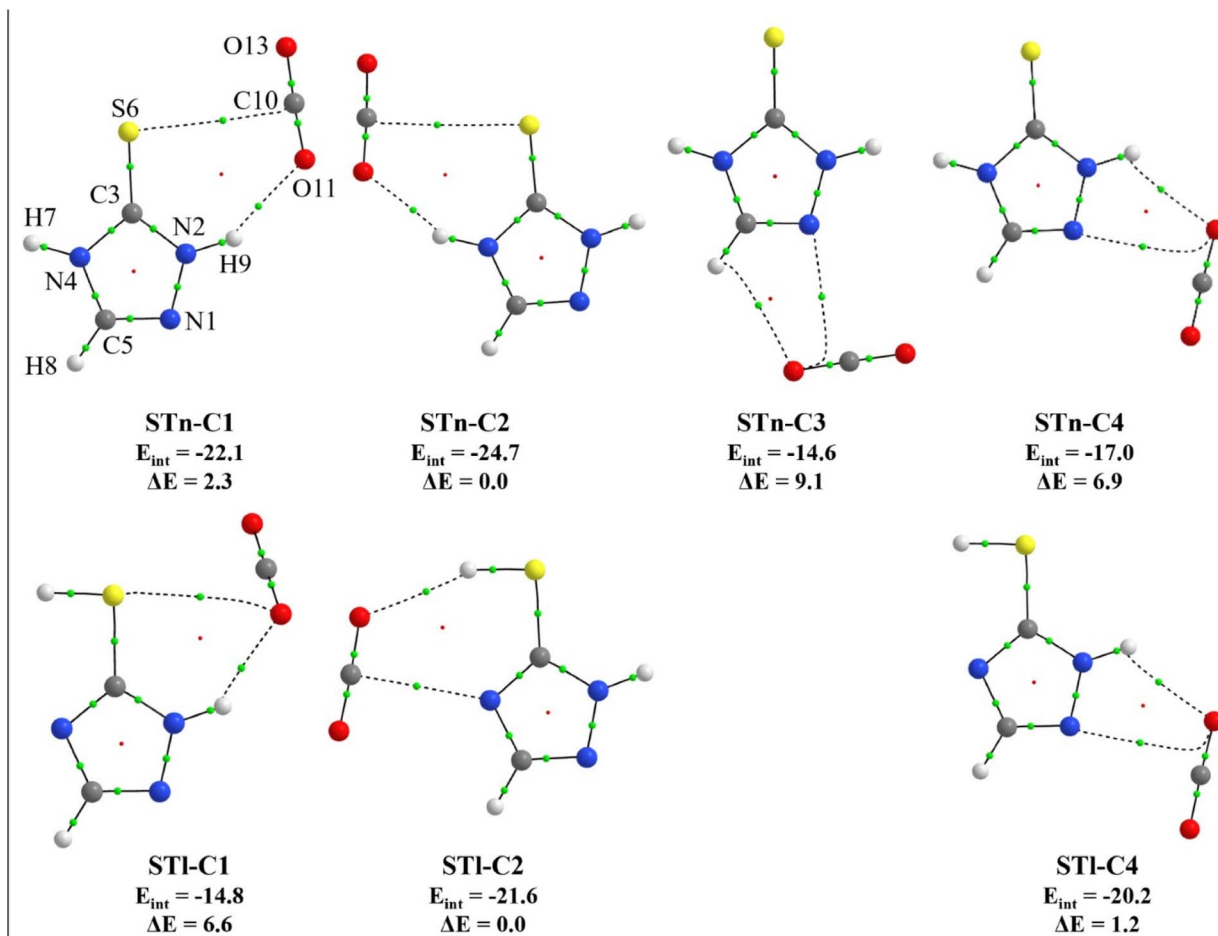


Fig. 2 Structures of 1 : 1 complexes of both ST tautomers with CO<sub>2</sub> molecule. Bond and ring critical points are marked with green and red dots, respectively. The values of interaction energy ( $E_{\text{int}}$ ) and relative electronic energy ( $\Delta E$ ) are given below the structures, both in kJ mol<sup>-1</sup>.

interactions involving two atoms of the CO<sub>2</sub> molecule (C10 and O11), while in the case of STI-C1, it is only an oxygen atom, whose electron density is distributed over two interactions. The next pair of structures are STn-C2 and STI-C2, which are also stabilized by two connections – a hydrogen bond and a van der Waals contact. Due to the presence of two NH groups in STn-C2, the subunits are linked by an N4–H7···O11 hydrogen bond and an additional S6···C10 interaction. In the case of STI-C2, it is an S6–H7···O11 hydrogen bond and an N4···C10 interaction. It is worth mentioning that these complexes turned out to be the most stable in their groups (thione and thiol tautomers). The structures STn-C4 and STI-C4 are characterized by the presence of a hydrogen bridge N1–H9···O11 and an additional N2···O11 connection. Both geometries are planar, and the NHO angle is 120.0 and 120.9°, respectively. Despite their very similar structure, the interaction energy values of these complexes differ by 4.2 kJ mol<sup>-1</sup> in favor of the STI-C4 form. The last of the optimized structures, STn-C3, is the least stable, with the interaction energy equal to –14.6 kJ mol<sup>-1</sup>. It is caused by the fact that, instead of the NH group, the CH group of the ring is involved in the interaction, forming a very weak hydrogen bond.

Worth mentioning is a certain relationship between the length of hydrogen bridges of individual structures and their

energetic stability. In the thione tautomer group, the most stable STn-C2 complex has a hydrogen bridge involving the N4–H group. The H7···O11 distance in this bridge is smaller than the analogous value of H9···O11 in the STn-C1 structure where the N2–H group is involved (2.093 Å compared to 2.149 Å, respectively). This suggests that the hydrogen bonds formed by the N4–H group are stronger than those formed by the N2–H group. This observation is consistent with the results of the structural analysis of ST complexes with N<sub>2</sub>.<sup>16</sup>

To better understand the origin of complex stability, we analyzed the hydrogen bond lengths and AIM topological parameters across all structures. The most stable complexes, STn-C2 and STI-C2, exhibit notably shorter N–H···O hydrogen bond distances and higher electron densities at the corresponding bond critical points, indicating stronger and more directional interactions. Furthermore, cooperative van der Waals contacts involving the sulfur atom (*e.g.*, S···C interactions) enhance stabilization by supporting the binding geometry. These features correlate well with the calculated interaction energies, highlighting the synergistic role of hydrogen bonding and dispersion forces in determining the relative stabilities of the complexes.



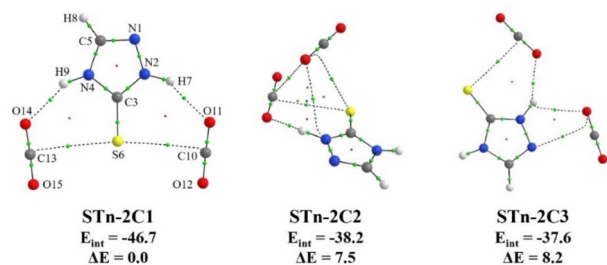


Fig. 3 Structures of 1 : 2 complexes of the STn tautomer with CO<sub>2</sub>. Bond, ring, and cage critical points are marked with green, red, and blue dots, respectively. The values of interaction energy ( $E_{\text{int}}$ ) and relative electronic energy ( $\Delta E$ ) are given below the structures, both in kJ mol<sup>-1</sup>.

**3.1.2. Complexes of the 1 : 2 stoichiometry.** Although the main goal of the study was to detect and analyze ST–CO<sub>2</sub> complexes of 1 : 1 composition, the formation of 1 : 2 aggregates could not be excluded under the experimental conditions used. The performed B3LYP-D3/6-311++G(3df,3pd) calculations revealed three stable structures formed between the ST thione tautomer and two CO<sub>2</sub> molecules. They are presented in Fig. 3, together with the values of interaction energy and relative energy.

Out of three 1 : 2 geometries, the most stable STn-2C1 is characterized by two hydrogen bonds: N2–H9...O11 and N4–H7...O14, as well as two additional stabilizing van der Waals interactions connecting the S6 atom with the C10 and C13 atoms of two CO<sub>2</sub> molecules. The H7...O14 distance in the hydrogen bridge formed by the N4–H group is smaller than the H9...O11 distance of the N2–H9...O11 bond (2.155 Å compared to 2.096 Å). This is consistent with the data obtained for ST

complexes with CO<sub>2</sub> of the 1 : 1 stoichiometry. In turn, the STn-2C2 and STn-2C3 complexes are characterized by higher energy values (by 7.5 and 8.2 kJ mol<sup>-1</sup>, respectively), as well as significantly lower interaction energies. The first one has an interesting geometry, in which, according to the AIM results, the arrangement of bond paths allowed for the formation of as many as four rings, which together form a cage. The AIM topological parameters of individual BCPs of the 1 : 2 structures, together with their selected geometric parameters, are available in Table S3 of the ESI.†

### 3.2. Matrix isolation infrared spectra of ST/CO<sub>2</sub>/Ar samples

In agreement with the previously published results<sup>16</sup> the ST monomers isolated in an argon matrix are present in the STn thione form (see Fig. 1). The introduction of the CO<sub>2</sub> dopant into the matrix gas resulted in the appearance of a series of bands that had not been present in the spectrum of ST in pure argon. To identify the particular geometries of the 1 : 1 complexes formed between ST and CO<sub>2</sub> in the matrix, positions of the new bands were compared with the theoretical wavenumbers calculated at the B3LYP-D3/6-311++G(3df,3pd) level. The values of the predicted band shifts of the four optimized 1 : 1 geometries (relative to the analogous monomer absorptions), together with their intensities and the corresponding experimental shifts, are summarized in Table 1.

Six selected fragments of the spectra of ST/CO<sub>2</sub>/Ar matrices are presented in Fig. 4 compared with the ST spectrum in pure argon. In the NH stretching mode range (3510–3430 cm<sup>-1</sup>), in addition to two intense absorptions caused by the  $\nu(\text{N}_2\text{H})$  and  $\nu(\text{N}_4\text{H})$  vibrations of the ST thione located at 3498.0 and 3491.0 cm<sup>-1</sup>, four new bands at lower wavenumbers appeared as a result of the complexation of the ST monomer with the CO<sub>2</sub>

**Table 1** Selected shifts of wavenumbers  $\Delta\nu$  (cm<sup>-1</sup>) and band intensities (km mol<sup>-1</sup>, in brackets) calculated at the B3LYP-D3/6-311++G(3df,3pd) level for the 1 : 1 complexes of the thione tautomer (STn) with a CO<sub>2</sub> molecule, compared with the experimental shifts

Theoretical shifts ( $\Delta\nu$ )				Mode <sup>16,a</sup>	Experimental shifts <sup>b</sup>	Assignment
STn-C1	STn-C2	STn-C3	STn-C4			
–10 (84)	–1 (104)	–1 (89)	–10 (67)	$\nu\text{N}_2\text{H}$	n.o.	
–29 (228)	–53 (249)	0 (103)	–7 (177)	$\nu\text{N}_4\text{H}$	–26.5	STn-C1
					–52.0	STn-C2
+1 (81)	+2 (61)	0 (50)	+2 (58)	$\nu\text{CN} + \delta\text{NH}$	+1.0	STn-C1
					+3.0	STn-C2
+4 (402)	+6 (430)	+1 (457)	+1 (507)	$\nu\text{CN} + \delta\text{NH} + \delta_{\text{ring}}$	+4.5, +6.0	STn-C1
					+7.0	STn-C2
+3 (15)	+5 (16)	–1 (21)	+1 (16)	$\nu\text{CN} + \delta_{\text{ring}}$	+7.0	STn-C2
					+9.0	STn-C1
–1 (77)	+3 (84)	+1 (100)	+1 (96)	$\nu\text{C} = \text{S} + \nu\text{CN} + \delta_{\text{ring}}$	–1.5	STn-C1
					+2.0	STn-C2
+4 (26)	+5 (34)	+4 (37)	+3 (42)	$\delta_{\text{ring}}$	+2.5	STn-C1
					+4.5	STn-C2
–33 (89)	–36 (64)	–15 (80)	–13 (71)	$\delta\text{CO}_2$	–17.0	STn-C1
					–19.0	STn-C2
+40 (81)	+65 (101)	+3 (138)	+16 (120)	$\gamma\text{NH} + \gamma_{\text{ring}}$	+28.5	STn-C1
					+30.5	STn-C2

<sup>a</sup> Abbreviations:  $\nu$  – bond stretching,  $\delta$  – in-plane bending,  $\gamma$  – out-of-plane bending. <sup>b</sup> Positions of the ST monomer bands: 3498.0, 3491.0, 1558.0, 1474.5, 1309.0, 1192.5, 932.5, 662.0, 566.0 cm<sup>-1</sup>.





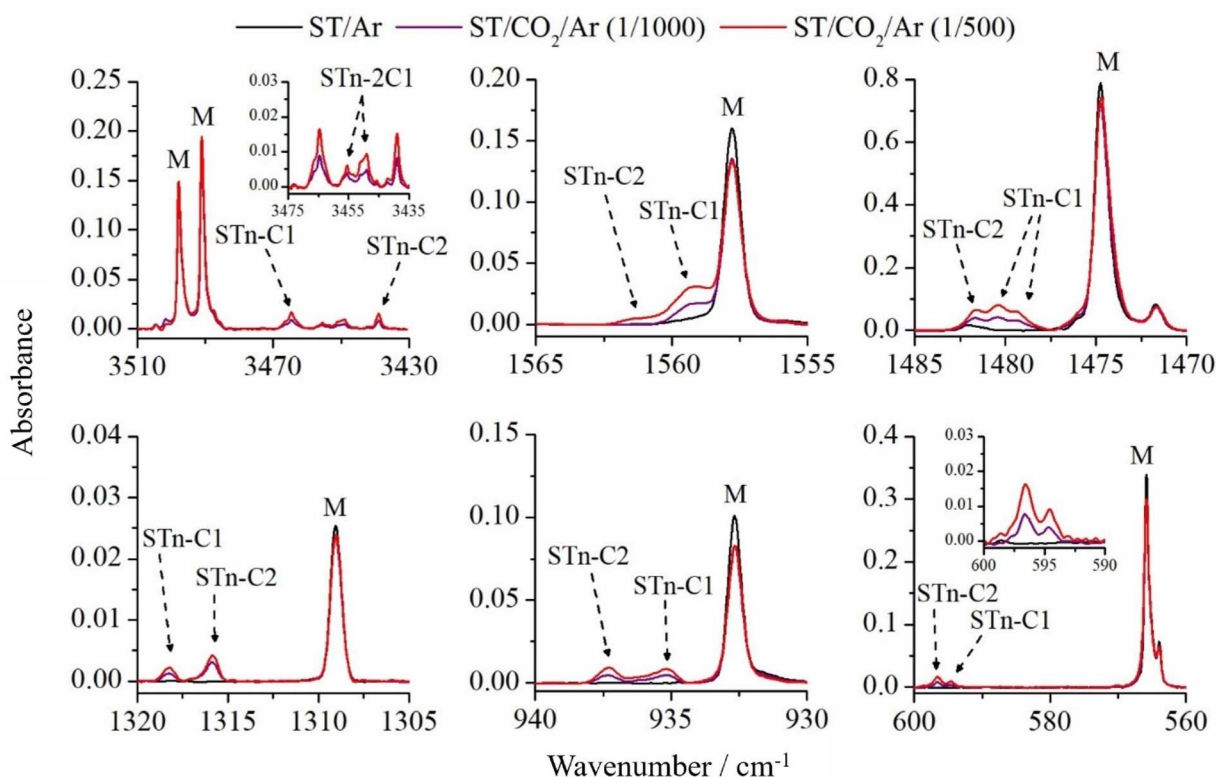


Fig. 4 Selected spectral ranges of ST/CO<sub>2</sub>/Ar matrices, where the CO<sub>2</sub>/Ar ratio was 1/500 (red line) and 1/1000 (purple line) and, for comparison, the spectrum of the ST/Ar matrix (black line). The letter M shows the ST monomer bands.

molecule. Two of them, at 3464.5 and 3439.0 cm<sup>-1</sup>, are characterized by a constant intensity ratio regardless of the CO<sub>2</sub> concentration in the system, which suggests that they can be assigned to 1 : 1 complexes. The observed wavenumber shifts relative to the STn monomer are equal to -26.5 and -52.0 cm<sup>-1</sup>. On the other hand, the doublet located at 3455.5/3449.0 cm<sup>-1</sup> is more intense at the CO<sub>2</sub>/Ar mixture concentration of 1/500. This most likely indicates the presence of aggregates of 1 : 2 stoichiometry.

Based on the results of DFT calculations, the two most stable 1 : 1 complexes of STn with CO<sub>2</sub>, namely STn-C1 and STn-C2, are characterized by -29 and -53 cm<sup>-1</sup> shifts in the  $\nu(\text{N}_4\text{H})$  stretching region, respectively. These values are in very good agreement with the experimental observation. Both geometries are characterized by the presence of the N-H...O hydrogen bridge and an additional S6...C10 interaction (see Fig. 2). In the remaining two STn...CO<sub>2</sub> complexes (STn-C3 and STn-C4), their NH groups do not participate in the formation of interactions with carbon dioxide, therefore their theoretical shifts of the  $\nu\text{N}_4\text{H}$  mode are much smaller (0 and -7 cm<sup>-1</sup>, respectively).

Other vibrations of the ST molecule are also sensitive to complexation, as shown in the remaining spectral regions of Fig. 4 and Table 1. In each region, new bands are present, shifted by a few cm<sup>-1</sup> towards higher wavenumbers, and their positions correspond to the predicted shifts for STn-C1 and STn-C2 species. In the range of 1485–1470 cm<sup>-1</sup>, containing the most intense band of the ST monomer originating from

complex stretching and deformation vibrations of the triazole ring, the band of the STn-C1 complex appears as a doublet separated by +4.5/+6.0 cm<sup>-1</sup>, and the third band (+7.0) can be assigned to the STn-C2 structure. In the remaining parts of the spectrum, the bands of both complexes appear as singlets. The observed shifts of the modes presented in Table 1 fit very well to the corresponding theoretical values obtained for ST-C1 and ST-C2 structures, indicating that both complexes are present in solid argon. It should be noted that the presence of the STn-C3 complex in the matrix cannot be completely ruled out because the DFT-predicted wavenumber shifts are, in many cases, very small or zero, and the bands originating from this structure can be obscured by the ST monomer peaks. On the other hand, much lower energetic stability of this form (9.2 kJ mol<sup>-1</sup> difference relative to the most stable complex) indicates that the formation of this structure is unlikely.

As mentioned earlier, two bands were also formed in the  $\nu\text{NH}$  range of the spectrum after deposition, which could be assigned to one of the complexes with stoichiometry higher than 1 : 1. To confirm this interpretation and to reveal more bands originating from these aggregates, the matrix temperature was increased to 32 K and cooled back to 10 K. A change in the intensity of the bands present in the spectrum and the appearance of new ones were observed. As shown in paragraph 3.1.2, the performed calculations reveal three STn...(CO<sub>2</sub>)<sub>2</sub> structures resulting from the addition of a second CO<sub>2</sub> molecule to the 1 : 1 complexes (see Fig. 2). Fig. 5 shows four spectrum

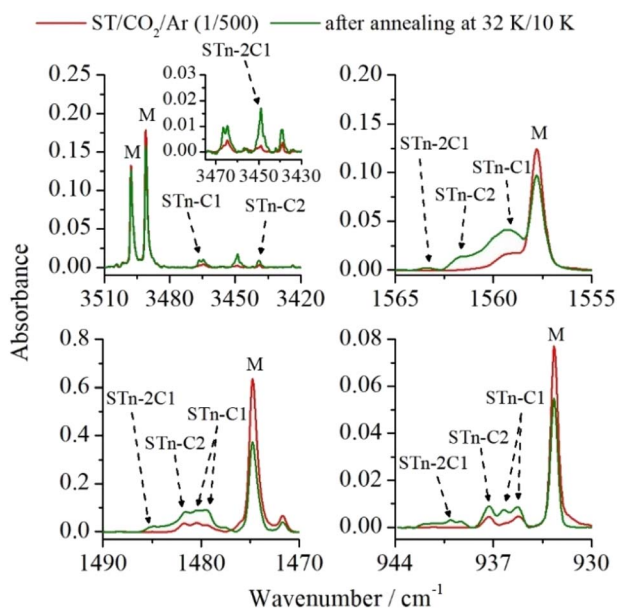


Fig. 5 Selected spectral ranges of ST/CO<sub>2</sub>/Ar matrices (CO<sub>2</sub>/Ar = 1/500) after deposition (red line) and after annealing the matrix to 32 K/10 K (green line). The letter M shows the ST monomer bands.

fragments, based on which the analysis and discussion on the structure of 1:2 complexes was carried out. The previously unassigned bands in the  $\nu$ NH range are located at 3445.5 and

3449.0 cm<sup>-1</sup>. Upon annealing, the latter was observed to increase its intensity more significantly, which allowed us to assume that both bands originate from the same structure isolated in two different matrix cavities. The second possibility is the presence of overlapping  $\nu$ N<sub>(2)</sub>H and  $\nu$ N<sub>(4)</sub>H bands of one of the 1:2 complexes. Comparison of the experimental and theoretical frequencies and intensities allowed us to conclude that the band located at 3449.0 cm<sup>-1</sup> comes from the  $\nu$ N<sub>(4)</sub>H vibration, and the other from the  $\nu$ N<sub>(2)</sub>H vibration of the STn-2C1 form. This is also confirmed by the fact that in other spectral ranges, no new absorptions were observed that could be assigned to another structure with the 1:2 composition. The data is available in Table S4 in the ESI.†

The described analysis at this point does not include complexes of the ST thiol tautomer. This is because this form is present in the matrix in a very small amount after deposition, and the observation of its complexes with the CO<sub>2</sub> molecule is impossible. However, information on the optimized STI...CO<sub>2</sub> structures, their geometry, energetics, and spectroscopic parameters (see paragraph 3.1.2.) are important in the context of the next paragraph, where the photoinduced tautomerization of STn and its complexes are discussed.

### 3.3. Photochemical generation of the thiol form STI complexes with CO<sub>2</sub>

Laser irradiation of matrices with UV light induced interesting changes in the ST/CO<sub>2</sub>/Ar spectra. Fig. 6 presents several regions

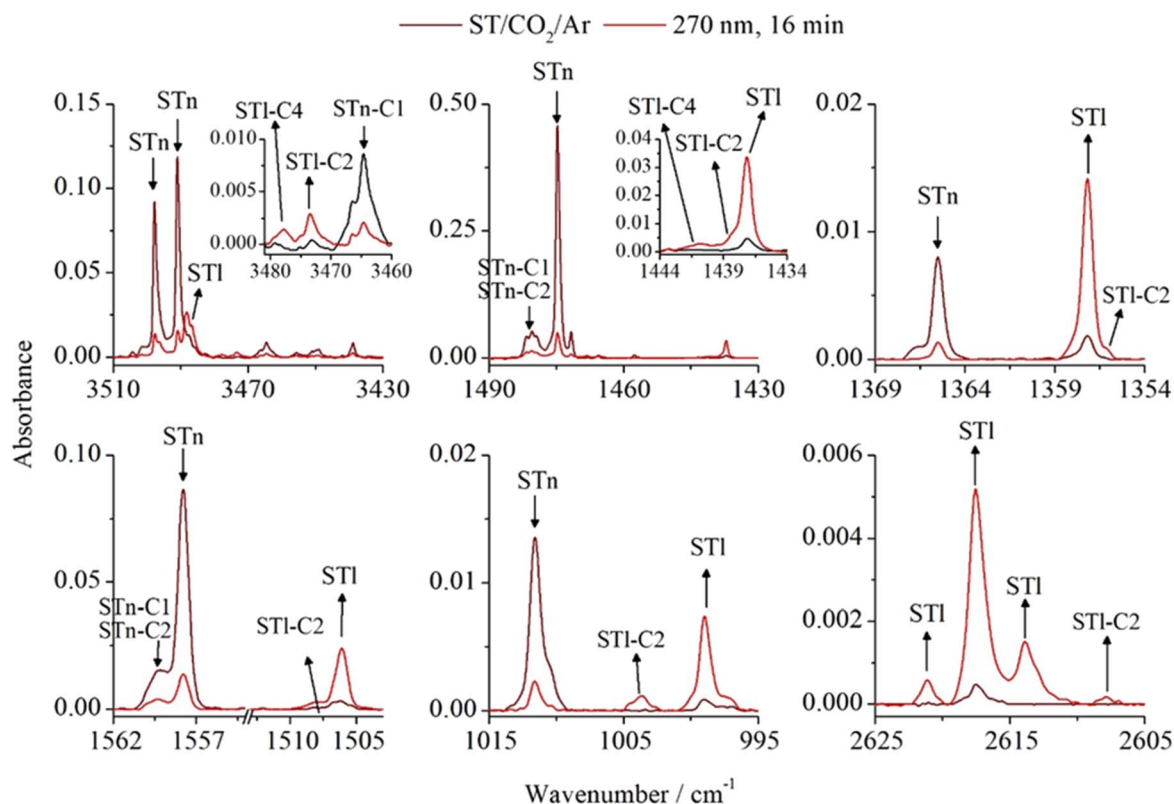


Fig. 6 Selected spectral ranges of the ST/CO<sub>2</sub>/Ar matrix (CO<sub>2</sub>/Ar = 1/500) after deposition (burgundy line) and after 16 min of irradiation with radiation of wavelength  $\lambda = 270$  nm (red line).



of the spectra obtained after 16 min irradiation at 270 nm compared to the spectrum of the matrix after deposition. The formation of the monomer thiol form STI as a result of tautomerization was accompanied by the appearance of additional bands in several spectral ranges. These bands were assigned to the complexes of the thiol form (STI...CO<sub>2</sub>), whose structures are presented in Fig. 2. Analyzing individual geometries, it could be predicted that the STn-C1 complex present in the matrix would transform into the STI-C1 form upon irradiation, as this process involves a change in the position of the hydrogen atom H7. In turn, irradiation of the STn-C2 complex will probably lead to the formation of the STI-C2, which is characterized by the lowest energy among all thiol STI...CO<sub>2</sub> complexes. However, despite the lack of the STn-C4 structure after deposition, the appearance of the STI-C4 structure under the influence of irradiation was also considered as a result of attaching a CO<sub>2</sub> molecule to the STI monomer formed in the matrix cavity.

The above considerations were assessed by comparing theoretical and experimental wavenumber shifts of the new bands (see Table 2), which are located near the analogous absorptions of the STI monomer. In the range of 3510–3430 cm<sup>−1</sup>, bands originating from the following structures are present before irradiation: STn-C1 (3464.5 cm<sup>−1</sup>), STn-C2 (3439.0 cm<sup>−1</sup>), and STn-2C1 (doublet at 3455.5/3449.0 cm<sup>−1</sup>). All of them decreased in intensity upon irradiation and, in addition to a band located at 3488.0 cm<sup>−1</sup> assigned to the STI monomer, a doublet appeared, which is shifted relative to the monomer by −10.0/−15.0 cm<sup>−1</sup>. These values correspond to the theoretical predictions for the νNH vibrations of the STI-C1 and STI-C4 complexes. The NH group of the third structure (STI-C2) is not involved in the interaction, therefore, the calculated νNH shift is equal to zero, and this band is not observed. In the range of 1490–1430 cm<sup>−1</sup>, where there are bands from complex stretching and deformation vibrations of the triazole ring, two new bands of low intensity appear. One of them occurs in the form of a shoulder on the STI monomer band (Δν = +1.0 cm<sup>−1</sup>), while the other is located away from the monomer absorption by +4.0 cm<sup>−1</sup>. These bands can be assigned to the STI-C2 and STI-C4 structures, respectively, based on the calculated shift values. The remaining spectral regions contain one new band

each, whose shifts best correspond to the values predicted for the STI-C2 structure. This suggests that this complex is predominant in the matrix after irradiation. It should also be mentioned that despite the presence of one STn geometry with a stoichiometry of 1 : 2 in the matrix after deposition, no bands were identified in the spectrum after irradiation that could originate from its thiol counterpart, most likely due to the low efficiency of photochemical conversion or a small amount of these species in the matrices.

### 3.4. Effect of ST complexation with CO<sub>2</sub> on the efficiency of thione–thiol tautomerization

Hydrogen atom transfer upon UV radiation is quite often observed in low-temperature matrices. In their latest review on this topic, Lapinski *et al.*<sup>19</sup> drew attention to the influence of matrix material on the H-atom transfer phenomenon. What is more, results of our recent paper on ST...N<sub>2</sub> complexes<sup>16</sup> showed that the efficiency of hydrogen atom transfer in ST complexed with N<sub>2</sub> is lower than in the monomeric form. Moving forward, it seemed interesting to investigate how the specific 1 : 1 interaction between STn and CO<sub>2</sub> influences the described thione → thiol transformation. For this purpose, the experimental integrated intensity ratios of the νN<sub>2</sub>H bands were determined for STn and STI monomers as well as for the STn-C2 and STI-C2 complexes. The ST/Ar and ST/CO<sub>2</sub>/Ar spectra recorded before and after 16 min of irradiation with radiation of λ = 270 nm were used. As can be seen in Table S5 (ESI),<sup>†</sup> the νN<sub>2</sub>H band intensity ratio equals 0.400 for monomers and 0.318 for complexes. Thus, the specific interaction of ST with the CO<sub>2</sub> molecule causes the transfer of the hydrogen atom in the complex to be about 20% less efficient than in the case of the monomer. This difference is smaller than in the case of the interaction with the nitrogen molecule, which indicates that despite the formation of stronger interactions between the ST and CO<sub>2</sub> subunits, they disturb the kinetics of the photochemical transformation to a lower extent. Changes in the concentration of individual monomers and complexes are presented in Fig. 7.

Analysis of the ST/Ar and ST/CO<sub>2</sub>/Ar spectra before and after irradiation revealed additional insights into how changes in bulk interactions, caused by the admixture of CO<sub>2</sub> in the argon

**Table 2** Selected shifts of wavenumbers Δν (cm<sup>−1</sup>) and band intensities (km mol<sup>−1</sup>, in brackets) calculated by the B3LYP-D3/6-311++G(3df,3pd) method for the 1 : 1 complexes of the thiol tautomer ST (STI) with a CO<sub>2</sub> molecule, compared with the experimental shifts. The values of the wavenumbers of the monomer bands, with respect to which the shifts were calculated, are given in brackets in the rightmost column

Theoretical shifts (Δν)			Mode <sup>16,a</sup>	Experimental shifts <sup>b</sup>	Assignment
STI-C2	STI-C4	STI-C1			
0 (87)	−16 (130)	−7 (147)	νN <sub>2</sub> H	−10.0 −15.0	STI-C2 STI-C4
−7 (48)	0 (8)	+1 (7)	νSH	−9.5	STI-C2
+2 (43)	−1 (52)	+1 (61)	νCN + δNH + δCN	+2.0	STI-C2
+2 (87)	+4 (131)	+2 (77)	νCN + δNH + δCN + δ <sub>ring</sub>	+4.0	STI-C2
+1 (36)	−3 (39)	−1 (37)	νCN + δ <sub>ring</sub>	−1.0	STI-C2
+4 (40)	+1 (59)	+2 (35)	δCN + δ <sub>ring</sub>	+4.5	STI-C2

<sup>a</sup> Abbreviations: ν – bond stretching, δ – in-plane bending. <sup>b</sup> Positions of the ST monomer bands: 3488.0, 2617.5, 1506.0, 1437.0, 1357.0, 999.0 cm<sup>−1</sup>.



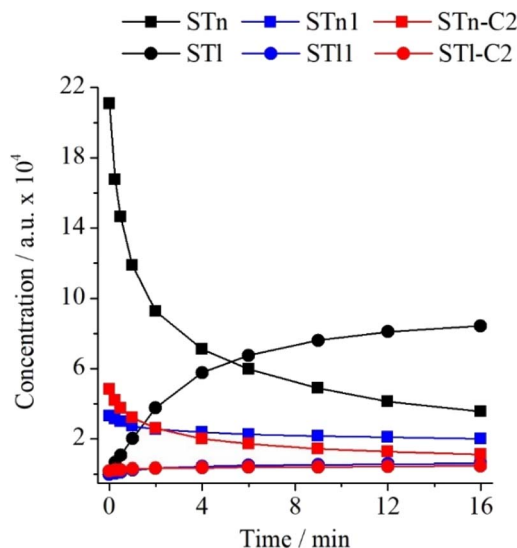


Fig. 7 Changes in the intensity of the  $\nu\text{N}_2\text{H}$  bands of ST monomers in the argon matrix and their complexes in the matrix doped with  $\text{N}_2$  or  $\text{CO}_2$  as a function of irradiation time at  $\lambda = 270$  nm.

matrix, affect the thione  $\rightarrow$  thiol transformation of the ST monomer. The intensity ratios calculated based on the spectra of the ST/Ar and ST/ $\text{CO}_2$ /Ar matrices ( $\text{CO}_2/\text{Ar} = 1/500$ ) are presented in Table S6 (ESI).<sup>†</sup> It presents that, in comparison to the nitrogen admixture, the presence of  $\text{CO}_2$  molecules in the STn environment has a less significant effect on the discussed photochemical reaction in the unbound ST. As shown in Fig. 8 below, one can notice that the decrease of STn and the simultaneous increase of STI are less substantial than in the case of the  $\text{N}_2$ -containing matrices.

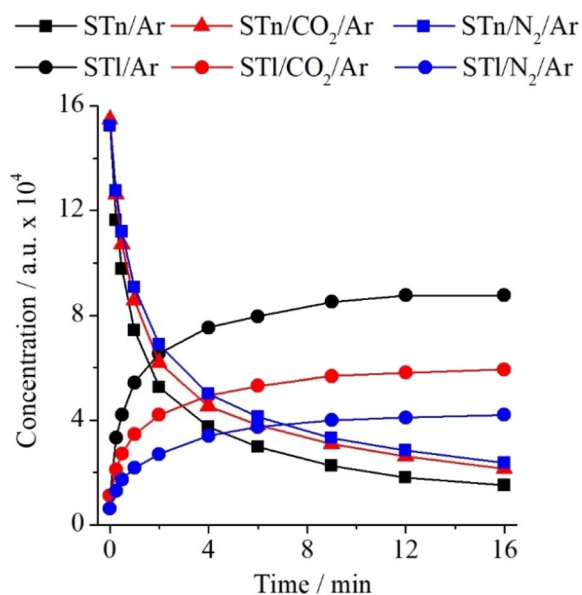


Fig. 8 Changes in the intensity of the most intense bands of STn and STI monomers ( $1474.5\text{ cm}^{-1}$  and  $1437.0\text{ cm}^{-1}$ , respectively) in ST/Ar, ST/ $\text{N}_2$ /Ar, and ST/ $\text{CO}_2$ /Ar matrices as a function of irradiation time at  $\lambda = 270$  nm.

## 4. Conclusions

Building on our previous work on 3-thio-1,2,4-triazole (ST) complexes with dinitrogen,<sup>16</sup> the study of ST complexes with carbon dioxide offers a compelling extension to explore the role of non-covalent interactions in atmospheric and environmental chemistry. Unlike  $\text{N}_2$ , which primarily interacts *via* weak van der Waals forces and specific hydrogen bonds,  $\text{CO}_2$ 's linear geometry and quadrupolar nature allow for diverse interaction modes, including  $\text{C}=\text{O}\cdots\text{H}$  hydrogen bonding and Lewis acid–base interactions with electron-rich sites on ST. Our findings reveal that the presence of  $\text{CO}_2$  in the matrix influences the photochemical behavior of ST, particularly its thione–thiol tautomerization. While both  $\text{N}_2$  and  $\text{CO}_2$  reduce the efficiency of this transformation compared to the isolated monomer, the effect of  $\text{CO}_2$  is notably less pronounced despite its stronger binding interactions. This suggests that the extent to which a gas-phase species modulates photochemical processes in low-temperature matrices depends not only on interaction energy but also on the geometry and specificity of intermolecular contacts. In this context, the current findings provide important insight into how  $\text{CO}_2$  modulates tautomerization *via* directional, non-covalent interactions. Although  $\text{ST}\cdots\text{CO}_2$  complexes exhibit stronger binding than their  $\text{N}_2$  counterparts, the reduction in tautomerization efficiency remains modest, underscoring that interaction geometry plays a more decisive role than energetic strength alone. Complexes such as STn-C2, stabilized by hydrogen bonds and  $\text{S}\cdots\text{C}$  van der Waals contacts, subtly hinder hydrogen transfer without entirely suppressing reactivity. These results highlight that photochemical reactivity in matrix-isolated systems is governed by the orientation and distribution of interactions, not solely their binding strength. Given the importance of  $\text{CO}_2$  in environmental chemistry and the growing interest in heterocyclic frameworks for  $\text{CO}_2$  capture, the findings presented here not only deepen our understanding of weak intermolecular forces but also shed light on  $\text{CO}_2$ -specific effects in photochemical and structural transformations of heterocycles. This study, therefore, expands the scope of previous investigations by demonstrating how differences in gas-matrix interactions can reshape molecular reactivity and photochemistry.

## Data availability

Data for this article, including spectra (.dat) and optimized structures (.log), are available at the Zenodo repository at <https://doi.org/10.5281/zenodo.15101158>.

## Author contributions

K. Mucha: conceptualization, methodology, data curation, investigation, visualization, writing – original draft, writing – review & editing. M. Pagacz-Kostrzewa: investigation, formal analysis, visualization; M. Wierzejewska: writing – original draft, supervision.





## Conflicts of interest

There are no conflicts to declare.

## Acknowledgements

Allocation of computer time from the Wrocław Centre for Networking and Supercomputing (Wrocław, Poland) is gratefully acknowledged. The authors thank Prof. Dr Małgorzata Biczysko for fruitful discussions concerning the theoretical part of this work.

## Notes and references

- 1 N. Veljkovic, S. Glisic, V. Perovic and V. Veljkovic, *Expet Opin. Drug Discov.*, 2011, **6**(12), 1263–1270, DOI: [10.1517/17460441.2012.638280](#).
- 2 P. O'Shea, *Biochem. Soc. Trans.*, 2003, **31**(5), 990–996, DOI: [10.1042/bst0310990](#).
- 3 D. Shah, B. Aldamzharov, A. Bukayeva, M. A. Torkmahalleh and G. Ahmadi, *Atmos. Environ.*, 2017, **166**, 334–339, DOI: [10.1016/j.atmosenv.2017.07.032](#).
- 4 A. A. Vigasin and I. I. Mokhov, *Izv. Atmos. Ocean. Phys.*, 2017, 164–173, DOI: [10.1134/S0001433817020116](#).
- 5 M. Paßens and S. Karthaus, *Surf. Sci.*, 2015, **642**, 11–15, DOI: [10.1016/j.susc.2015.07.025](#).
- 6 A. V. Desai, S. Sharma, S. Let and S. K. Ghosh, *Coord. Chem. Rev.*, 2019, **395**, 146–192, DOI: [10.1016/j.ccr.2019.05.020](#).
- 7 J.-P. Zhang, Y.-B. Zhang, J.-B. Lin and X.-M. Chen, *Chem. Rev.*, 2012, **112**(2), 1001–1033, DOI: [10.1021/cr200139g](#).
- 8 W.-L. Cao, Q. Tariq, Z.-M. Li, J.-Q. Yang and J.-G. Zhang, *Def. Technol.*, 2022, **18**(3), 344–367, DOI: [10.1016/j.dt.2021.12.002](#).
- 9 Y. Shao, Y. Jiang, D. Wang, B. Guo, J. Zhao, Z. Zhou, J. Chen, R. Guo, Y. Lei and L. Jin, *Fuel*, 2024, **375**, 132534, DOI: [10.1016/j.fuel.2024.132534](#).
- 10 K. Wang, Z. Zhang, S. Wang, L. Jiang, H. Li and C. Wang, *ChemSusChem*, 2024, **17**(16), e202301951, DOI: [10.1002/cssc.202301951](#).
- 11 M. R. Aouad, M. Messali, N. Rezki, M. A. Said, D. Lentz, L. Zubaydi and I. Warad, *J. Mol. Struct.*, 2019, **1180**, 455–461, DOI: [10.1016/j.molstruc.2018.12.010](#).
- 12 K. Anichina, A. Mavrova, D. Yancheva, J. Tsenov and R. Dimitrov, *J. Mol. Struct.*, 2017, **1150**, 179–187, DOI: [10.1016/j.molstruc.2017.08.073](#).
- 13 P. V. Bharatam, O. R. Valanju, A. A. Wani and D. K. Dhaked, *Drug Discovery Today*, 2023, **28**(4), 103494, DOI: [10.1016/j.drudis.2023.103494](#).
- 14 F. Mesiti, A. Maruca, V. Silva, R. Rocca, C. Fernandes, F. Remião, E. Uriarte, S. Alcaro, A. Gaspar and F. Borges, *Eur. J. Med. Chem.*, 2021, **213**, 113183, DOI: [10.1016/j.ejmech.2021.113183](#).
- 15 A. Boruah, B. Boro, J. Wang, R. Paul, R. Ghosh, D. Mohapatra, P.-Z. Li, X. Zhang and J. Mondal, *ACS Appl. Mater. Interfaces*, 2025, **17**(1), 1259–1272, DOI: [10.1021/acsami.4c17714](#).
- 16 K. Mucha, M. Pagacz-Kostrzewa and M. Wierzejewska, *J. Photochem. Photobiol., A*, 2023, **443**, 1–8, DOI: [10.1016/j.photochem.2023.114873](#).
- 17 M. J. Nowak, I. Reva, H. Rostkowska and L. Lapinski, *Phys. Chem. Chem. Phys.*, 2017, **19**, 11447–11454, DOI: [10.1039/c7cp01363a](#).
- 18 L. Lapinski, M. J. Nowak and H. Rostkowska, *J. Chem. Phys.*, 2017, **146**(9), 094306, DOI: [10.1063/1.4977604](#).
- 19 L. Lapinski, H. Rostkowska and M. J. Nowak, *Int. Rev. Phys. Chem.*, 2022, **41**, 1–47, DOI: [10.1080/0144235X.2022.2030613](#).
- 20 M. J. Frisch, G. W. Trucks, H. B. Schlegel, G. E. Scuseria, M. A. Robb, J. R. Cheeseman, G. Scalmani, V. Barone, G. A. Petersson, H. Nakatsuji, X. Li, M. Caricato, A. V. Marenich, J. Bloino, B. G. Janesko, R. Gomperts, B. Mennucci, H. P. Hratchian, J. V. Ortiz, A. F. Izmaylov, J. L. Sonnenberg, D. Williams Young, F. Ding, F. Lipparini, F. Egidi, J. Goings, B. Peng, A. Petrone, T. Henderson, D. Ranasinghe, V. G. Zakrzewski, J. Gao, N. Rega, G. Zheng, W. Liang, M. Hada, M. Ehara, K. Toyota, R. Fukuda, J. Hasegawa, M. Ishida, T. Nakajima, Y. Honda, O. Kitao, H. Nakai, T. Vreven, K. Throssell, J. A. Montgomery Jr, J. E. Peralta, F. Ogliaro, M. J. Bearpark, J. J. Heyd, E. N. Brothers, K. N. Kudin, V. N. Staroverov, T. A. Keith, R. Kobayashi, J. Normand, K. Raghavachari, A. P. Rendell, J. C. Burant, S. S. Iyengar, J. Tomasi, M. Cossi, J. M. Millam, M. Klene, C. Adamo, R. Cammi, J. W. Ochterski, R. L. Martin, K. Morokuma, O. Farkas, J. B. Foresman and D. J. Fox, *Gaussian 16, Revision C.01*, Gaussian, Inc., Wallingford CT, 2016.
- 21 R. Dennington, T. A. Keith and J. M. Millam, *GaussView, Version 6.1*, Semichem Inc., Shawnee Mission, KS, 2016.
- 22 S. Grimme, J. Antony, S. Ehrlich and H. Krieg, *J. Chem. Phys.*, 2010, **132**, 1–19, DOI: [10.1063/1.3382344](#).
- 23 S. Grimme, S. Ehrlich and L. Goerigk, *J. Comput. Chem.*, 2011, **32**, 1456–1465, DOI: [10.1002/jcc.21759](#).
- 24 A. D. McLean and G. S. Chandler, *J. Chem. Phys.*, 1980, **72**, 5639–5648, DOI: [10.1063/1.438980](#).
- 25 K. Raghavachari, J. S. Binkley, R. Seeger and J. A. People, *J. Chem. Phys.*, 1980, **72**, 650–654, DOI: [10.1063/1.438955](#).
- 26 S. Grimme, S. Ehrlich and L. Goerigk, *J. Comput. Chem.*, 2011, **32**, 1456–1465, DOI: [10.1002/jcc.21759](#).
- 27 S. F. Boys and F. Bernardi, *Mol. Phys.*, 1970, **19**, 553–566, DOI: [10.1080/00268977000101561](#).
- 28 S. Simon, M. Duran and J. J. Dannenberg, *J. Chem. Phys.*, 1996, **105**, 11024–11031, DOI: [10.1063/1.472902](#).
- 29 R. F. W. Bader, *Atoms in Molecules: A Quantum Theory*, Oxford University Press, Oxford, UK, 1990.
- 30 R. F. W. Bader, *Chem. Rev.*, 1991, **91**, 893–928, DOI: [10.1021/cr00005a013](#).
- 31 T. A. Keith, *TK Gristmill Software*, AIMAll (Version 19.10.12), Overland Park KS, USA, 2019.
- 32 K. Mucha and M. Wierzejewska, *Spectrochim. Acta, Part A*, 2024, **313**, 1–9, DOI: [10.1016/j.saa.2024.124127](#).
- 33 H. Rostkowska, L. Lapinski and M. J. Nowak, *J. Phys. Chem. A*, 2017, **121**, 6932–6941, DOI: [10.1021/acs.jpca.7b05621](#).